A reliable, noninvasive technique for spindle imaging and enucleation of mammalian oocytes

Lin Liu[1,2], Rudolf Oldenbourg[2], James R. Trimarchi[1,2], and David L. Keefe[1,2]*

[1]*Department of Ob/Gyn, Women and Infants Hospital, Brown University, Providence, RI 02905.* [2]*Marine Biological Laboratory, Woods Hole, MA 02543.*
Corresponding author (Dkeefe@smtp.wihri.org).

Factors affecting the efficiency of animal cloning remain to be elucidated[1,2]. Enucleation of recipient oocytes is a critical step in cloning procedures and typically is performed by aspirating a portion of the cytoplasm underlying the first polar body. Enucleation is evaluated using epifluorescence after Hoechst staining for DNA[3–6], which may disrupt functions of the cytoplast, especially mitochondria[7]. Mitochondrial DNA in Dolly and other cloned sheep has been shown to derive exclusively from recipient oocytes[8]. Not only might evaluation of the aspirated karyoplast portion[5] inadequately reflect the state of the cytoplast, it is also time consuming. Here we report a reliable, noninvasive technique for spindle imaging and enucleation of oocytes using a new microscope, the Pol-Scope[9]. The efficiency of enucleation was 100%, and only 5.5% of the oocytes' mitochondria entered the karyoplast upon Pol-Scope-directed removal of the spindle. Moreover, Pol-Scope imaging of spindles and micromanipulation did not compromise the developmental competence of reconstituted oocytes and cytoplasts.

In mature oocytes, chromosomes are aligned over the metaphase plate of the meiotic spindle. Because spindles are highly birefringent[10], they can be observed directly with a polarized light microscope[10,11]. Observations of spindles are limited by the orientation dependence of conventional polarized light microscopy, which employs plane-polarized light. Thus spindle fibers with their slow axis not oriented appropriately to the plane-polarized light cannot be imaged properly. The new Pol-Scope incorporates liquid crystals with electro-optical control and software, and employs circular-polarized light to image birefringent structures, regardless of sample orientation, thus facilitating quantitative analysis of birefringent structures[9,12]. Layers of birefringence in the zona pellucida of hamster oocytes were first reported using this new technology[13]. Pol-Scope imaging allows efficient observation of the meiotic spindles in oocytes from different mouse strains (C57B6, CF-1, CD-1, and B6C3F1) and golden hamsters (Fig. 1). The location of the spindle relative to the polar body varied among mouse oocytes, as described previously for hamsters[14], which may explain the suboptimal efficiency of current enucleation methods using the polar body as an indicator. We removed spindles by micromanipulation from oocytes collected from CD-1 or B6C3F1 mice. In three independent experiments, 30, 24, and 33 oocytes were enucleated by spindle removal using the Pol-Scope (Fig. 1D, E, F). Chromosomal DNA, stained with Hoechst 33342, was aligned on spindles in all karyoplasts (Fig. 1G, H). In contrast, no cytoplasts (n = 87) exhibited DNA staining,
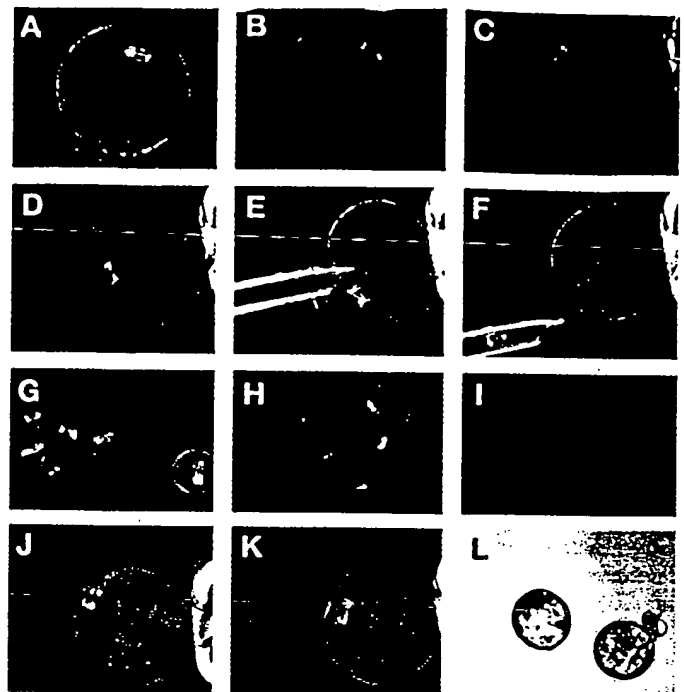

Figure 1. The use of the Pol-Scope for spindle imaging, spindle removal-directed enucleation, and reconstitution of metaphase II oocytes. Pol-Scope imaging of meiotic spindles (indicated by arrow) in (A) a C57B6 and (B) CF-1 mouse oocyte, and (C) hamster oocyte. Removal of spindle from a CD1 mouse oocyte aided by the Pol-Scope: The meiotic spindle, indicated by arrow, before (D), during (E), and after (F) removal and enucleation with a beveled pipette. Confirmation of spindle removal and enucleation by Hoechst stain (10 µg ml⁻¹) of nuclear DNA for 10 min and fluorescence microscopy: (G) Karyoplasts imaged with the Pol-Scope before staining, and (H) corresponding karyoplasts showing DNA stain under UV exposure. (I) An enucleated cytoplast without nuclear DNA. Reconstitution and development of B6C3F1 mouse oocytes: (J) Couplet of cytoplast and karyoplast before fusion and (K) 1 h after fusion, viewed using the Pol-Scope. (L) Blastocysts developed from the fused oocytes after IVF. Bar (A-K) = 30 µm; Bar (L) = 100 µm.

demonstrating enucleation efficiency with the Pol-Scope of 100%. Furthermore, only 5.5% of mitochondria, estimated by integrated mitochondrial fluorescence density after MitoTracker Red staining, were removed with the karyoplast.

To investigate further the developmental capacity of cytoplasts created under Pol-Scope imaging, we assessed the development of parthenogenetically activated, reconstituted oocytes collected from B6C3F1 mice (Fig. 1J, K). The rate of cleavage and development to blastocysts did not differ (P > 0.05) between oocytes reconstituted after Pol-Scope-directed enucleation (Spindle NT) and control oocytes never subjected to the Pol-Scope imaging and micromanipulation (Act control; Table 1). Moreover, the total cell number and the number of apoptotic cells in developed blastocysts did not differ between the two groups (P > 0.05). We also examined the develop-

Figure 2. Pol-Scope imaging of metaphase II spindles (indicated by arrowheads) of a bovine oocyte (A) free of zona pellucida and (B) with zona pellucida intact. (C) Metaphase II spindle of a human oocyte, imaged with the Pol-Scope.

Table 1. Parthenogenetic development in vitro of reconstituted B6C3F1 mouse oocytes*

Groups	Number of oocytes	Number (%) cleaved at Day 2	Number (%) blastocysts at Day 4	Cell number in blastocysts (means ± s.d.)	
				Total	Apoptotic
Spindle NT	68	61 (90)	53 (78)	45.0 ± 7.1	1.0 ± 1.2
Act control	79	68 (86)	56 (71)	46.3 ± 7.6	1.0 ± 0.7

*Oocytes derived from spindle and chromosome transfer (Spindle NT) and nonmanipulated, nonimaged oocytes (Act control), activated by electroporation followed by 6-DMAP incubation.

ment of reconstituted oocytes after in vitro fertilization (IVF). A low proportion of reconstituted oocytes were fertilized in vitro, probably because electroporation-induced fusion affected their fertilizability. However, successfully fertilized zygotes cleaved and developed at a frequency similar to that of control oocytes that had not undergone micromanipulation and imaging (data not shown). The morphology (Fig. 1L) and the cell number of developed blastocysts were comparable to controls.

As the current efficiency of cloning by nuclear transfer is extremely low, and many other factors undoubtedly complicate the development of cloned embryos[2], it was not feasible to test the viability of the cytoplasts using the nuclear transfer procedure itself. Alternatively, we compared the development after IVF of the Pol-Scope-imaged versus nonimaged B6C3F1 mouse oocytes. Before and during the Pol-Scope imaging, oocytes were incubated in HKSOM containing 2 µg/ml cytochalasin D for 1 h to mimic the micromanipulation environment. Results showed that the Pol-Scope-imaged oocytes ($n = 77$) cleaved (73%) and developed to blastocysts (66%) at similar rates ($P > 0.05$) to those (75% and 70%, respectively) of control oocytes ($n = 80$), without being subjected to the Pol-Scope imaging. To further test the viability of blastocysts developed after Pol-Scope imaging of oocyte spindles and IVF, 47 blastocysts were transferred into four pseudopregnant CD-1 foster females. In one foster, blastocysts transferred were derived from micromanipulated oocytes under the direction of Pol-Scope, from which a small amount of cytoplasm, but not the spindle, was removed. All fosters became pregnant and delivered 33 (70%) live offspring. This rate of development to term was comparable to that (75%) of in vivo-developed blastocysts, not exposed to the Pol-Scope imaging, in which a total of 108 blastocysts were transferred and 81 healthy pups were produced. Therefore, Pol-Scope imaging of oocyte spindles did not affect full development of manipulated oocytes and thus is truly noninvasive. The noninvasiveness of Pol-Scope imaging was not unexpected because the light intensity at the specimen was not different from that produced by Nomarski DIC optics (~60 µW).

Our experiments indicate that the Pol-Scope can image noninvasively the meiotic spindle and be employed to achieve an enucleation efficiency rate of 100% in rodent oocytes. Moreover, only small amounts of cytoplasm, with few mitochondria, are removed with the spindle-karyoplast. The remaining cytoplasmic volume is critical for further normal development after reconstruction[15,16]. This noninvasive, reliable technique for preparation of cytoplasts should improve the efficiency of cloning, and should be especially beneficial for cloning of endangered and rare species, whose donor oocytes are especially valuable. Although Nomarski imaging produces a faint outline of the spindle and metaphase plate in oocytes from a few mouse strains[17], such optics cannot identify meiotic spindles in most species, including sheep, cattle, and pig, and most other mouse strains[6,18]. However, we have been able to image meiotic spindles of bovine and human metaphase II oocytes using the Pol-Scope and found that the high lipid contents exhibited low birefringence and did not interfere with spindle imaging in bovine oocytes using the Pol-Scope (Fig. 2). We also imaged spindles of B6C3F1 mouse oocytes (Fig. 1D), in which many granule lipids were observed. Latham and

Solter (1993) suggested that conventional polarized-light microscopy might be useful for oocyte enucleation, but never reported data in support of this hypothesis[19]. We not only demonstrate here the utility and the noninvasive property of the Pol-Scope to direct enucleation and probably facilitate a new procedure (spindle transfer), but we also report the application of the new Pol-Scope to provide orientation-independent images of the spindle with high resolution.

Experimental protocol

Oocyte collection, enucleation, and Pol-Scope imaging. Two- to three-month-old mice or golden hamsters were induced to superovulate by consecutive injection of PMSG and hCG. Cumulus–oocyte complexes were collected from oviduct ampullae following hCG injection. Cumulus cells were removed from the oocytes by gentle pipetting after mild incubation with 0.03% hyaluronidase in HEPES-buffered potassium simplex optimized medium (HKSOM). Denuded oocytes were washed in HKSOM and incubated in normal KSOM, supplemented with nonessential amino acids[20], pending enucleation or IVF. Enucleation of oocytes was performed in HKSOM containing 2 µg/ml cytochalasin D under an inverted microscope (Zeiss Axiovert 100TV, New York, NY), equipped with Pol-Scope optics, a liquid crystal control instrument (Cambridge Medical Instrumentatin, Boston MA), MetaMorph Pol-Scope Imaging Software (Universal Imaging Corporation, Boston, MA), and with Narishige micromanipulators (Tokyo, Japan). The working principle and usage of the Pol-Scope has been described[12,13]. For a batch of oocytes, calibrating the Pol-Scope requires 1-1.5 min. Imaging an individual oocyte spindle requires an average of 14 s. The computerized retardance image was used to direct removal of the spindle (Fig. 1B). Mitochondria in intact oocytes, cytoplasts, and karyoplasts were labeled with 330 nM MitoTracker Red (Molecular Probes, Eugene, OR) for 15 min, and images were digitally obtained and recorded. The integrated fluorescence density was calculated with the MetaMorph software. Staining of mitochondria was used to estimate the approximate amount of cytoplasm and mitochondria removed.

In vitro fertilization of mouse oocytes, embryo culture, and embryo transfer. In vitro fertilization (IVF) of denuded B6C3F1 mouse oocytes occurred in TYH medium, as described[15]. After IVF, oocytes were washed and cultured in 50 µl droplets of KSOM under mineral oil at 37°C in a humidified atmosphere of 7% CO₂ in air. Subsequent cleavage at day 2 (fertilization day defined as day 1) and development to blastocyst stage at day 4 were examined. Some blastocysts were transferred surgically into uterus horns of pseudopregnant CD-1 foster females that had been mated with vasectomized CD-1 males three days previously. To establish the efficiency of embryo transfer, blastocysts developed in vivo were flushed from uteri of B6C3F1 at day 4 and then transferred into CD-1 fosters, as described above.

Reconstitution of oocytes by electrofusion, and oocyte activation. Karyoplasts were inserted under the zona pellucida (Fig. 1D: j), then reconstituted by electrofusion, induced by a single DC pulse of 1.0 kV cm⁻¹ for 40 µs in the fusion medium (0.28 M mannitol, added with 0.1 mM MgSO₄ and 2 mM histidine⁴). Reconstituted oocytes were activated by electroporation with a single DC pulse in the fusion medium, added with 0.1 mM CaCl₂, followed by incubation in 5 mM 6-dimethylaminopurine (DMAP) for 2.5 h. Oocytes were washed and cultured as above. The TUNEL assay was employed to determine apoptotic cells, using the In Situ Cell Death Detection Kit (Boehringer-Mannheim, Indianapolis, IN), and propidium iodide to assess the total cell number in developed blastocysts.

Acknowledgments

1. Robl, JM. Development and application of technology for large scale cloning of cattle. *Theriogenology* 51, 499–508 (1999).
2. Campbell, K.H.S. Nuclear equivalence, nuclear transfer, and the cell cycle. *Cloning* 1, 3–15 (1999).
3. Cibelli, J.B. et al. Cloned transgenic calves produced from nonquiescent fetal fibroblasts. *Science* 280, 1256–1258 (1998).
4. Liu, L. Dai, Y. & Moor, R.M. Nuclear transfer in sheep embryos: the effect of cell-

BEST AVAILABLE COPY

cycle coordination between nucleus and cytoplasm and the use of in vitro matured oocytes. *Mol. Reprod. Dev.* **47**, 255–264 (1997).

5. Wilmut, I., Schnieke, A.E., McWhir, J., Kind, A.J. & Campbell, K.H.S. Viable offspring derived from fetal and adult mammalian cells. *Nature* **385**, 810–813 (1997).

6. Cheong, H.T., Takahashi, Y. & Kanagawa, H. Relationship between nuclear remodeling and subsequent development of mouse embryonic nuclei transferred to enucleated oocytes. *Mol. Reprod. Dev.* **37**, 138–145 (1994).

7. Smith, L.C. Membrane and intracellular effects of ultraviolet irradiation with Hoechst 33342 on bovine secondary oocytes matured in vitro. *J. Reprod. Fertil.* **99**, 39–44 (1993).

8. Evans, M.J. et al. Mitochondrial DNA genotypes in nuclear transfer-derived cloned sheep. *Nat. Genet.* **23**, 90–93 (1999).

9. Oldenbourg, R. A new view on polarization microscopy. *Nature* **381**, 811–812 (1996).

10. Inoue, S. Polarization optical studies of the mitotic spindle. I. The demonstration of spindle fibers in living cells. *Chromosoma* **5**, 487–500 (1953).

11. Hiramoto, Y. et al. Quantitative studies on the polarization optical properties of living cells. II. The role of microtubules in birefringence of the spindle of the sea urchin egg. *J. Cell Biol.* **89**, 121–130 (1981).

12. Oldenbourg, R. Polarized light microscopy of spindles. *Methods Cell Biol.* **61**, 175–208 (1999).

13. Keefe, D., Tran, P., Pellegrini, C. & Oldenbourg, R. Polarized light microscopy and digital image processing identify a multilaminar structure of the hamster zona pellucida. *Human Reprod.* **12**, 1250–1252 (1997).

14. Silva, C.P., Kommineni, K., Oldenbourg, R. & Keefe, D.L. The first polar body does not predict accurately the location of the metaphase II meiotic spindle in mammalian oocytes. *Fertil. Steril.* **71**, 719–721 (1999).

15. Wakayama, T. & Yanagimachi, R. Fertilisability and developmental ability of mouse oocytes with reduced amounts of cytoplasm. *Zygote* **6**, 341–346 (1998).

16. Peura, T.T., Lewis, I.M. & Trounson, A.O. The effect of recipient oocyte volume on nuclear transfer in cattle. *Mol. Reprod. Dev.* **50**, 185–191 (1998).

17. Wakayama, T., Perry, A.C.F., Zuccotti, M., Johnson, K.R. & Yanagimachi, R. Full-term development of mice from enucleated oocytes injected with cumulus cell nuclei. *Nature* **394**, 369–374 (1998).

18. Tsunoda, Y., Shioda, Y., Onodera, M., Nakamura, K. & Uchida, T. Differential sensitivity of mouse pronuclei and zygote cytoplasm to Hoechst staining and ultraviolet irradiation. *J. Reprod. Fertil.* **82**, 173–178 (1988).

19. Latham, K.E.L. & Solter, D. Transplantation of nuclei to oocytes and embryos. *Methods Enzymol.* Vol. 225, 719–732 (1993).

20. Liu, Z. & Foote, R.H. Effects of amino acids on the development of in-vitro matured in-vitro fertilized bovine embryos in a simple protein-free medium. *Human Reprod.* **10**, 2985–2991 (1995).

A colorimetric assay for rapid screening of antimicrobial peptides

Sofiya Kolusheva, Laurent Boyer, and Raz Jelinek

Department of Chemistry, Ben Gurion University of the Negev, Beersheva 84105, Israel.

The increased resistance of various bacteria toward available antibiotic drugs has initiated intensive research efforts into identifying new sources of antimicrobial substances. Short antibiotic peptides (10–30 residues) are prevalent in nature as part of the intrinsic defense mechanisms of most organisms and have been proposed as a blueprint for the design of novel antimicrobial agents[1]. Antimicrobial peptides are generally believed to kill bacteria through membrane permeabilization and extensive pore-formation[1]. Assays providing rapid and easy evaluation of interactions between antimicrobial membrane peptides and lipid bilayers could significantly improve screening for substances with effective antibacterial properties, as well as contribute to the elucidation of structural and functional properties of antimicrobial peptides. Here we describe a colorimetric sensor in which particles composed of phospholipids and polymerized polydiacetylene (PDA) lipids were shown to exhibit striking color changes upon interactions

with antimicrobial membrane peptides. The color changes in the system occur because of the structural perturbation of the lipids following their interactions with antimicrobial peptides. The assay was also sensitive to the antibacterial properties of structurally and functionally related peptide analogs.

Phospholipid–PDA vesicles were prepared through sonication of the aqueous mixtures of the phospholipid and 10,12-tricosadiynoic acid (4:6 mole ratio) at a temperature of –70°C, followed by slow cooling overnight and irradiation at 254 nm (ref. 2). The vesicles exhibited an intense blue color due to the alternating conjugated triple bond/double bond PDA backbone[3]. Figure 1 shows a portion of a 96-well plate containing polymerized dimiristoylphosphocholine (DMPC)–PDA vesicle solutions into which identical quantities of the membrane-associated antibiotic peptides melittin[4], magainin II[5], and alamethicin[6], as well as the soluble neuropeptide hormone PBAN[7], were added separately. These results demonstrate that addition of the membrane peptides led to color changes within the vesicle solutions. Peptides that are not expected to bind cellular membranes do not induce detectable colorimetric transitions, as shown, for example, in a mixture consisting of the vesicles and the neuropeptide PBAN (Fig. 1E). No colorimetric responses (negative controls) have been detected for various other soluble peptides and proteins that generally appear in physiological solutions, such as albumin. The different degrees of color changes induced by each peptide most likely depend upon their distinctive modes of interactions with the DMPC/PDA vesicle interface.

Previous studies have revealed that biological processes leading to structural perturbations at the PDA vesicle interface, including ligand–receptor recognition[8], pH changes[9], and enzymatic catalysis[2], are responsible for the blue-red transitions occurring in the vesicle assemblies. Specifically, the color changes are caused by strains induced in the conjugated backbone of the PDA vesicles following rearrangements of the pendant side chains of the PDA molecules[10,11]. A similar mechanism most likely accounts for the colorimetric transitions that occur in the phospholipid–PDA vesicles following addition of the membrane peptides. Binding of the peptides gives rise to extensive molecular reorganization within the phospholipid domains[8,12], affecting the structure of the surrounding PDA matrix, which results in the blue-red color changes.

We carried out further experiments to evaluate the sensitivity of the technique and the dependence of the color change upon the type of phospholipids included within the PDA matrix. Titration curves in Figure 2A depict the colorimetric responses (CR) of the phospholipid–PDA vesicles as a function of the concentration of melittin. The CRs were calculated from the relative blue and red absorbances detected in the UV-visible spectra, and provide a quantitative value of the blue-red transitions[8]. The results shown in Figure 2A indicate that addition of melittin induced color changes in PDA assemblies incorporating DMPC, dimiristoylphosphoethanolamine (PE), and in mixtures of PE and dimiristoylphosphatidylglycerol (PG), and cardiolipin. Low CR was detected upon addition of melittin to pure PDA vesicles (no incorporated phospholipids). This residual CR, due to nonspecific interactions between the PDA vesicles and melittin, was treated as a "background" in the analysis of the assay results (see discussion below).

The titration curves (Fig. 2A) demonstrate the applicability of the assay using a variety of lipid components. It is important to note that PE, PG, and cardiolipin, rather than phosphocholine derivatives, are the primary constituents of bacterial membranes[13]. As this figure also indicates, the highest colorimetric sensitivity to melittin is found in PE–PDA vesicles—a result that is most likely due to the smaller headgroup of PE, which facilitates easier interaction of the peptide with the lipid interior.

The titration curves of melittin (Fig. 2A) reveal that the phospholipid–PDA vesicles could detect melittin even in micromolar concentrations (e.g., a CR of <20% would be perceived as a distinct